Dilepton production at RHIC and LHC

M. A. Betemps[a], M. B. Gay Ducati[b], **E. G. de Oliveira**[b]

[a] Conjunto Agrotécnico Visconde da Graça, Universidade Federal de Pelotas, Caixa Postal 460, 96060-290 Pelotas, RS, Brazil
[b] Instituto de Física, Universidade Federal do Rio Grande do Sul, Caixa Postal 15051, 91501-970 Porto Alegre, RS, Brazil

In a recent work[1], Drell-Yan dilepton production at backward rapidities in hadrons collisions was studied in the rest frame of the target, i. e., in the color dipole approach. In this work, we compare these previous results with results obtained using the well known intrinsic k_T approach in the infinite momentum frame [2, 3] (IMF). The dilepton production is of particular interest since dileptons do not interact strongly and therefore carry information about initial state effects. We compare both formalisms in proton-nucleus collisions at backward rapidities (proton as a target) at RHIC and LHC energies. The results show qualitative agreement between the two formalisms through the nuclear modification ratio as a function of both rapidity and transverse momentum and also show that low-mass dileptons are relevant observables to probe nuclear effects.

Drell–Yan process in the IMF

In the IMF frame, the Drell-Yan process is understood as the combination of two partons to create a virtual boson that subsequently splits in the dilepton. For dilepton mass M much smaller than the Z mass, the dominant process includes only the photon as the virtual boson. In the kinematics used here partons and hadrons are taken as massless, the momenta of hadrons A and B are P_A and P_B, and the longitudinal momenta of partons are $p_A = x_A P_A$ and $p_B = x_B P_B$. The virtual photon momentum is q, and $q^2 = M^2$ is the squared dilepton mass. The Mandelstam variables are given by: $s = 2P_A \cdot P_B$, $t = (q - P_A)^2$, and $u = (q - P_B)^2$. We also define $x_1 = 2P_B \cdot q/s$, $x_2 = 2P_A \cdot q/s$, and the photon (longitudinal) rapidity $y = \frac{1}{2}\ln(x_1/x_2)$. It can be showed that:

$$x_{1,2} = \sqrt{\frac{M^2 + p_T^2}{s}} \mathrm{e}^{\pm y}, \tag{1}$$

in which p_T is the photon (also dilepton) transverse momentum.

We consider then partonic intrinsic transverse momentum, i. e., partons are not collinear to hadrons [2, 3]. The partonic distributions are modified as the following prescription:

$$f(x)dx \to f(x)h(\vec{k_T})dxd^2k_T. \tag{2}$$

In this paper, we consider $h(\vec{k_T}) = \frac{1}{2\pi b^2}\exp\left(\frac{k_T^2}{2b^2}\right)$. Therefore, the cross section is given by[4, 5]:

$$\sigma_S(s, M^2, y, p_T) = h'(p_T^2)\frac{d\sigma}{dM^2 dy} + \int d^2q_T \sigma_P(s, M^2, q_T^2)[h'((\vec{p}_T - \vec{q}_T)^2) - h'(p_T^2)]. \tag{3}$$

In the above expression, it is included the NLO collinear double differential cross section:

$$\frac{d\sigma}{dM^2 dy} = \frac{\hat{\sigma}_0}{s}\int_0^1 dx_A dx_B dz \delta(x_A x_B z - \tau)\delta\left(y - \frac{1}{2}\ln\frac{x_A}{x_B}\right) \times \left\{P_{q\bar{q}}(x_A, x_B, M^2)\left[\delta(1-z) + \frac{\alpha_s(M^2)}{2\pi}D_q(z)\right] + P_{qg+gq}(x_A, x_B, M^2)\left[\frac{\alpha_s(M^2)}{2\pi}D_g(z)\right]\right\}.$$

Using the modified minimal subtraction scheme ($\overline{\mathrm{MS}}$), $D_q(z)$ and $D_g(z)$ are given e.g. in Ref. [6] ($C_F = 4/3$, $T_R = 1/2$).

The second term in the right hand side of equation 3 is calculated only from annihilation and Compton diagrams and is written as[4]:

$$\sigma_P(s, M^2, p_T^2) = \frac{1}{\pi^2}\frac{\alpha^2\alpha_s}{M^2\hat{s}^2}\int_{x_{A\min}}^1 dx_A \frac{x_B x_A}{x_A - x_1}\left\{P_{q\bar{q}}(x_A, x_B, M^2)\frac{8}{27}\frac{2M^2\hat{s} + \hat{u}^2 + \hat{t}^2}{\hat{t}\hat{u}} + P_{qg}(x_A, x_B, M^2)\frac{1}{9}\frac{2M^2\hat{u} + \hat{s}^2 + \hat{t}^2}{-\hat{s}\hat{t}} + P_{gq}(x_A, x_B, M^2)\frac{1}{9}\frac{2M^2\hat{t} + \hat{s}^2 + \hat{u}^2}{-\hat{s}\hat{u}}\right\}$$

in which $x_{A\min}$ is given by $(x_1 - \tau)/(1 - x_2)$, $x_B = (x_A x_2 - \tau)/(x_a - x_1)$, and $P_{q\bar{q}}(x_A, x_B) = \sum_q e_q^2\left(f_q(x_A)f_{\bar{q}}(x_B) + \bar{q} \leftrightarrow q\right)$; $P_{qg}(x_A, x_B) = \sum_q e_q^2\left(f_q(x_A) + f_{\bar{q}}(x_A)\right)f_g(x_B)$; $P_{gq}(x_A, x_B) = \sum_q e_q^2 f_g(x_A)\left(f_q(x_B) + f_{\bar{q}}(x_B)\right)$.

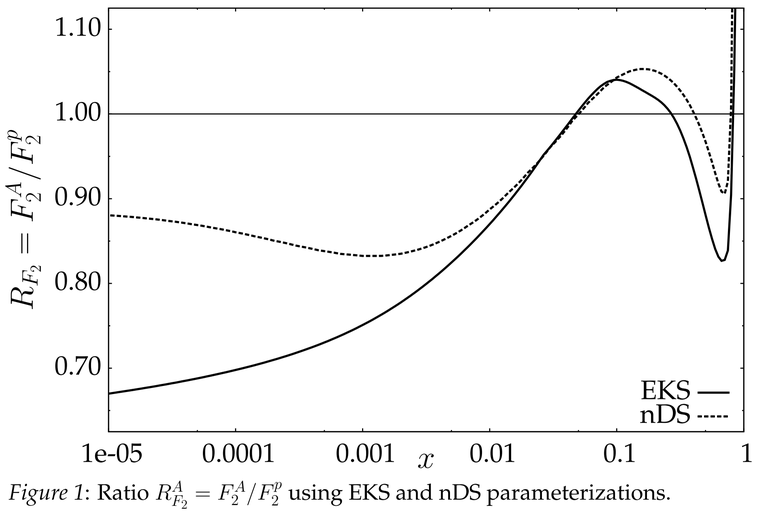

Figure 1: Ratio $R_{F_2}^A = F_2^A/F_2^p$ using EKS and nDS parameterizations.

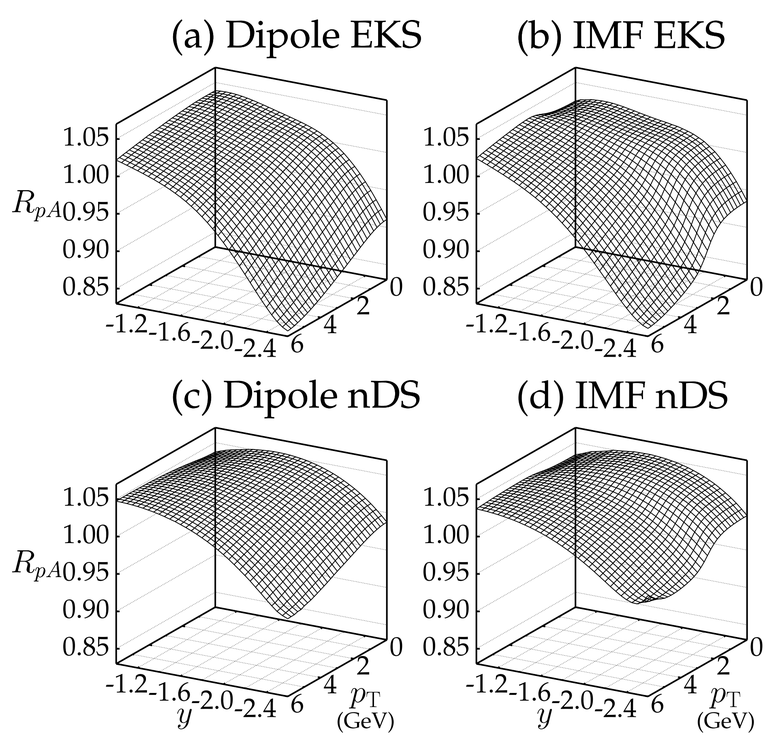

Figure 2: Factor R_{pA} at RHIC energies ($\sqrt{s} = 200$ GeV) as a function of rapidity and transverse momentum.

Color dipole picture of Drell–Yan

In the color dipole approach, Drell–Yan dilepton production is studied in the rest frame of the target. So, the projectile emits a quark (or antiquark), which fluctuates into a state of quark–photon and interacts with the color field of the target, and the photon is freed to split into a dilepton. The color dipole cross section arises as the interference of the diagram in which the quark first interacts with the target with the diagram in which the quark first fluctuates in the quark–photon state. This result was first stated in [7] and derived in detail in [5].

In [1], the color dipole approach was used to study dileptons produced at backward rapidities, so the proton was considered as the target and the nucleus as the projectile. In this case, the color dipole approach is phenomenologically valid for small x_1[5] – very backward rapidities. The cross section is written as:

$$\frac{d\sigma^{DY}}{dM^2 dy d^2p_T} = \frac{\alpha_{em}^2}{6\pi^3 M^2}\int_0^\infty d\rho W(x_2, \rho, p_T)\sigma_{\mathrm{dip}}(x_1, \rho), \tag{4}$$

in which ρ is the dipole transverse size. In this case, x_2 is the projectile momentum fraction carried by the virtual photon.

The weight function $W(x_2, \rho, p_T)$ contains the nuclear structure function $F_2^A(x_2/\alpha, M^2) = \sum_q e_q^2[x f_q^A(x, M^2) + x f_{\bar{q}}^A(x, M^2)]$:

$$W(x_2, \rho, p_T) = \int_{x_2}^1 \frac{d\alpha}{\alpha^2}F_2^A(\frac{x_2}{\alpha}, M^2)\left\{[m_q^2\alpha^4 + 2M^2(1-\alpha)^2]\left[\frac{1}{p_T^2 + \eta^2}T_1(\rho) - \frac{1}{4\eta}T_2(\rho)\right] + [1 + (1-\alpha)^2]\left[\frac{\eta p_T}{p_T^2 + \eta^2}T_3(\rho) - \frac{1}{2}T_1(\rho) + \frac{\eta}{4}T_2(\rho)\right]\right\},$$

in which $\eta^2 = (1-\alpha)M^2 + \alpha^2 m_q^2$ and $m_q = 0,2$ GeV is the quark mass. The functions T_i are given by: $T_1(\rho) = \frac{\rho}{\alpha}J_0\left(\frac{p_T\rho}{\alpha}\right)K_0\left(\frac{\eta\rho}{\alpha}\right)$, $T_2(\rho) = \frac{\rho^2}{\alpha^2}J_0\left(\frac{p_T\rho}{\alpha}\right)K_1\left(\frac{\eta\rho}{\alpha}\right)$, and $T_3(\rho) = \frac{\rho}{\alpha}J_1\left(\frac{p_T\rho}{\alpha}\right)K_1\left(\frac{\eta\rho}{\alpha}\right)$, in which $J_n(x)$ is the Bessel function of the first kind and $K_n(x)$ is the modified Bessel function of the second kind.

We use the model introduced by Golec-Biernat and Wüsthoff (GBW)[8] for the dipole cross section:

$$\sigma_{dip}(x, r) = \sigma_0\left[1 - \exp\left(-\frac{r^2 Q_0^2}{4(x/x_0)^\lambda}\right)\right], \tag{5}$$

in which $Q_0^2 = 1$ GeV^2 and there are three fitted parameters: $\sigma_0 = 23,03$ mb (59,14 GeV^{-2}), $x_0 = 3,04 \times 10^{-4}$, and $\lambda = 0,288$. It is important to highlight that the present dipole cross section includes saturation effects, not included in the IMF approach.

PDFs

We use GRV98[9, 10] as the parton distribution function (PDF) of free protons. Two parameterizations of the nuclear PDFs are used: EKS[11, 12, 13] and nDS[14]. EKS parameterization gives the nPDF as the free proton PDF multiplied by a factor: $f_q^A(x, Q) = R_q^A(x, Q)f_q^p(x, Q)$, while nDS gives the nPDF as a convolution of the free proton PDF and a weight function:

$$f_q^A(x, Q) = \int_x^A \frac{dy}{y}W_q(y, A)f_q^p\left(\frac{x}{y}, Q\right). \tag{6}$$

EKS parameterization is available only at leading order, while nDS is also at NLO. In Fig. 1, both parameterizations are compared at leading order calculating $R_{F_2}^A = F_2^A/F_2^p$. We would like to stress that nDS parameterization presents lower ratio for most values of x studied, in particular for EMC ($0.3 < x < 0.8$) and shadowing ($x < 0.1$) effects – other regions correspond to anti-shadowing ($0.1 < x < 0.3$) and Fermi motion ($0.8 < x$) effects.

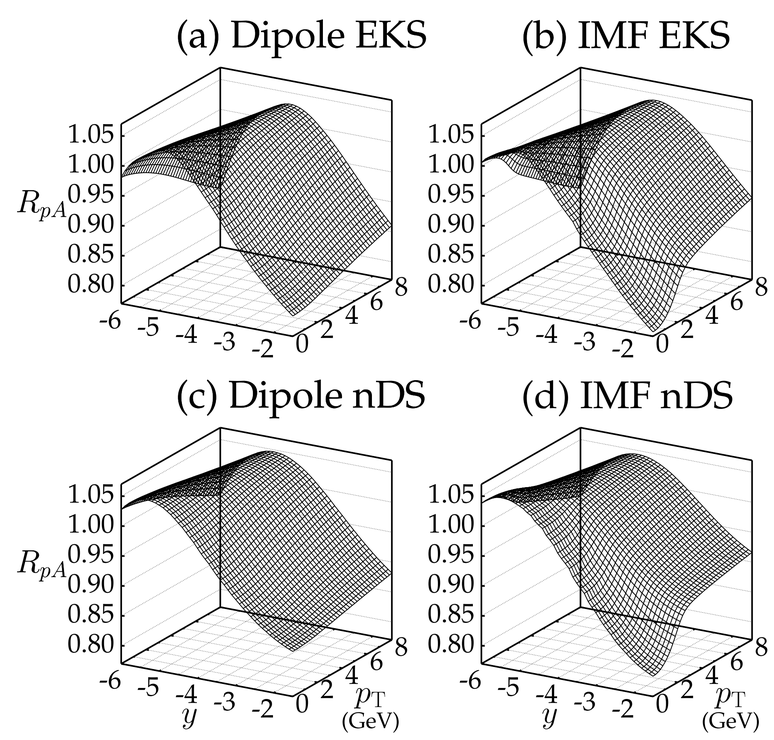

Figure 3: Factor R_{pA} at LHC energies ($\sqrt{s} = 8800$ GeV) as a function of rapidity and transverse momentum.

Results

We use dilepton mass of $M = 6.5$ GeV, gold nucleus ($A = 196.97$), and intrinsic k_T standard deviation of $b = 0.48$ GeV. In Figs. 2 and 3, the nuclear modification factor:

$$R_{pA} = \frac{d\sigma(pA)}{dp_T^2 dy dM}\Big/ A\frac{d\sigma(pp)}{dp_T^2 dy dM} \tag{7}$$

is calculated for RHIC and LHC energies. The main difference among formalisms is a step near $p_T = 2.5$ GeV in the IMF distributions, caused by the different ways that the two terms in Eq. 3 take into account nuclear effects, since each is dominant in one region of p_T. This result shows that saturation effects included in the dipole approach are not very effective in changing the nuclear modification ratio.

For RHIC energies, the behavior of R_{pA} is mainly explained by the inclusion of anti-shadowing effects with decreasing x_2 approximately from 0.64 ($y = -2.6, p_T = 7$) to 0.09 ($y = -1.0, p_T = 0$). Anti-shadowing effects are characterized by an increase in the nuclear cross section, exactly what is seen in Fig. 2. For LHC energies (Fig. 3), shadowing effects are also important, represented by a decrease after the increase caused by anti-shadowing as x_2 decreases. EKS and nDS parameterizations give qualitatively similar results, showing that both approaches roughly give the same dependence of R_{pA} on the nuclear effects. EKS parameterization predicts a smaller R_{pA} than nDS parameterization in both approaches and nDS parameterization shows more sensitivity to the approach.

In conclusion, we show that low-mass dileptons are relevant in probing nuclear effects at RHIC energies. The results obtained showed strong dependence on the nuclear effects. Among the approaches, qualitative agreement was obtained in the nuclear modification factor, showing that saturation effects (considered in the color dipole formalism) do not play a key role in this factor. However, the nuclear modification factor proved to be very sensitive to the introduction of an intrinsic transverse momentum, given the step seen in the p_T distribution.

This work is partially supported by CNPq.

References

[1] M. A. Betemps, M. B. Gay Ducati, and E. G. de Oliveira, Phys. Rev. **D74**, 094010 (2006), hep-ph/0607247.

[2] G. Altarelli, G. Parisi, and R. Petronzio, Phys. Lett. **B76**, 351 (1978).

[3] G. Altarelli, G. Parisi, and R. Petronzio, Phys. Lett. **B76**, 356 (1978).

[4] R. D. Field, *Applications of Perturbative QCD*, Frontiers in Physics Vol. 77 (Addison-Wesley, Redwood City, 1989).

[5] J. Raufeisen, J.-C. Peng, and G. C. Nayak, Phys. Rev. **D66**, 034024 (2002), hep-ph/0204095.

[6] R. K. Ellis, W. J. Stirling, and B. R. Webber, *QCD and Collider Physics*, Camb. Monogr. Part. Phys. Nucl. Phys. Cosmol. Vol. 8 (Cambridge University, Cambridge, 1996).

[7] B. Kopeliovich, Soft component of hard reactions and nuclear shadowing, in *Workshop Hirschegg'95: Dynamical Properties of Hadrons in Nuclear Matter*, edited by H. Feldmeier and W. Nörenberg, pp. 102–112, Darmstadt, 1995, GSI, hep-ph/9609385.

[8] K. J. Golec-Biernat and M. Wusthoff, Phys. Rev. **D59**, 014017 (1999), hep-ph/9807513.

[9] M. Gluck, E. Reya, and A. Vogt, Eur. Phys. J. **C5**, 461 (1998), hep-ph/9806404.

[10] M. Gluck, E. Reya, and A. Vogt, Z. Phys. **C67**, 433 (1995).

[11] K. J. Eskola, V. J. Kolhinen, and P. V. Ruuskanen, Nucl. Phys. **B535**, 351 (1998), hep-ph/9802350.

[12] K. J. Eskola, V. J. Kolhinen, and C. A. Salgado, Eur. Phys. J. **C9**, 61 (1999), hep-ph/9807297.

[13] K. J. Eskola, V. J. Kolhinen, H. Paukkunen, and C. A. Salgado, JHEP **05**, 002 (2007), hep-ph/0703104.

[14] D. de Florian and R. Sassot, Phys. Rev. **D69**, 074028 (2004), hep-ph/0311227.